Diblock Copolymer Microemulsions. A Scaling Model

N. Dan[†] and M. Tirrell*

Department of Chemical Engineering and Material Science, University of Minnesota, Minneapolis, Minnesota 55455

Received August 5, 1992; Revised Manuscript Received October 26, 1992

ABSTRACT: The properties of diblock copolymers as emulsifiers of immiscible and highly selective solvents are investigated using a scaling model. Solvent selectivity leads to copolymer aggregation at the liquid–liquid interface and the formation of stable microdomains. We find that symmetrical copolymers form lamellae at all copolymer concentrations. Asymmetrical copolymers, however, aggregate in spherical microdomains at equilibrium with the two bulk solvent phases. The interface curvature and the surface density increase, and the volume of the emulsion phase volume decreases, with the copolymer degree of asymmetry. The critical aggregation concentration is found to be significantly lower than the critical micelle concentration (cmc). The emulsion phase volume increases linearly with copolymer concentration, until, when one of the solvents is exhausted, cylindrical domains appear. At high copolymer concentrations lamellae replace the cylindrical droplets.

I. Introduction

Emulsions are dispersions of two immiscible liquids, characterized by small, but finite, domain size. As a rule, they are thermodynamically unstable. The addition of surface-active agents leads to thermodynamic stability of the system and allows control of domain size and geometry.

Diblock copolymers, due to their amphiphilic nature, are the macromolecular analogue of small-molecule surfactants. In mixtures of two immiscible and inversely selective solvents, namely, solvents in which one block is miscible but the other is not, the copolymer chains are driven to the liquid–liquid interface by the unfavorable interactions between incompatible solvent–block pairs.[1,2] The effective interfacial tension is thereby reduced, at the cost of a loss in entropy and an increase in chain stretching energy. The balance between the interfacial energy and chain elasticity determines the polymer density at the interface.[3] When the initial, macroscopic, interface between the two immiscible solvents is saturated by copolymer chains, new interfaces form. As a result, stable, equilibrium microdomains separated by polymer interfacial layers appear and a microemulsion is obtained (see Figure 1). The total interface area is set by the initial volume fraction of copolymer and the surface density, or the number of chains per unit area.

Understanding the relationship between copolymer structure and the microemulsion phase properties is important. Unlike short-chain surfactants, copolymers can be manufactured, in principle, to suit any immiscible liquid mixture. The control of domain size and geometry, afforded by comparatively small adjustments in copolymer composition or concentration, would enable tailoring the emulsion phase to answer specific needs. Also, microdomains formed by macromolecular surfactants are more stable against thermal fluctuations and coagulation than those of their small-molecule counterparts.

The emulsified liquids need not be small-molecule solvents. It has been shown[1] that the addition of appropriately chosen copolymers to homopolymer blends significantly lowers the effective interfacial tension and leads to formation of stable microdomains.[4] The properties of such emulsions were calculated by Wang and Safran,[5] and Leibler,[6] where phase morphology was determined as a function of copolymer asymmetry and system composition.

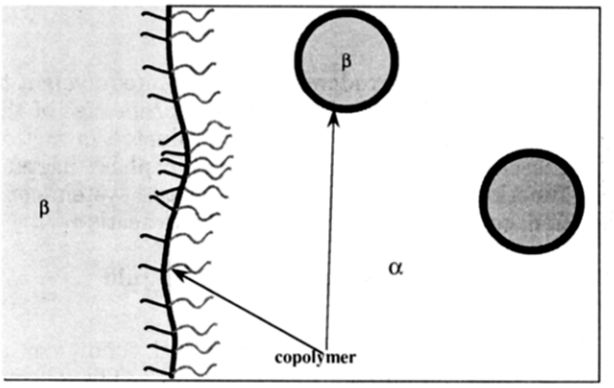

Figure 1. Diblock copolymer as emulsifier of immiscible solvents. The two liquids phase separate, forming a macroscopic interface. The copolymer is driven to the interface, thereby reducing the interfacial tension. Copolymer asymmetry leads to local interface curvature and, eventually, the formation of droplets. The total interface area is determined by the copolymer concentration and the equilibrium surface density.

However, the properties of polymers in bulk are quite different from those of polymers in solution, so that these results cannot be directly applied to emulsions of small-molecule solvents.

The structures of diblock lamellae[7] and spherical microdomains[8,9] in mixtures of immiscible small-molecule solvents have been studied, using mean-field[7,9] and self-consistent-field[8] (SCF) models. Assuming a single, specific domain geometry, their validity is limited to a narrow range of copolymer asymmetry and concentration. In the case of spherical domains, the necessity of a numerical solution further restricts predictions to the specific parameters chosen.

In this study we explore the full equilibrium phase diagram of monodisperse diblock copolymers as emulsifiers of immiscible and selective solvents. We use a scaling model[10–13] to describe the copolymer interfacial layer, emphasizing the effect of interface curvature on the configurations of the constituent chains. The analysis of the copolymer interface properties, namely, curvature and surface density, enables determination of microdomain morphology as a function of diblock asymmetry and system composition.

The paper is organized as follows: In section II we investigate the properties of a single interface, at equilibrium with two bulk solvents. The critical copolymer

[†] Department of Materials and Interfaces, Weizmann Institute of Science, Rehovot 76100, Israel.

0024-9297/93/2226-0637$04.00/0

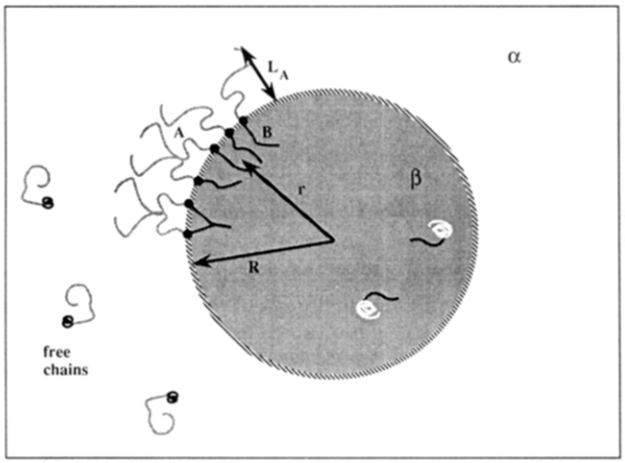

Figure 2. Diblock copolymers at liquid–liquid interfaces. The copolymer aggregates at the interface, the A block forming a brush in α solvent and the B block a brush in β solvent. The B block is shorter than A and is therefore located on the concave side of the interface. Free chains are distributed throughout both solvent phases, adopting a collapsed globule–solvated corona configuration.

concentration for microdomain formation (equivalent to the cmc in micellar solutions) and the properties of the emerging microemulsion phase are evaluated in section III. In section IV we derive the equilibrium phase diagram, as a function of copolymer asymmetry and system composition, concluding with a discussion in section V.

II. Diblock Copolymers at Liquid–Liquid Interfaces

We consider a monodisperse AB diblock copolymer, in a mixture of two immiscible solvents, α and β. The solvents are inversely selective, so that α is a precipitant for the B block and a good solvent for the A block, and β inversely so. The unfavorable interaction energy between incompatible block–solvent pairs drives copolymer chains to the liquid–liquid interface, thereby reducing the effective interfacial tension. The stretching energy of the copolymer blocks, which increases with copolymer density, counteracts this tendency. The balance between the two driving forces determines the equilibrium surface density and the interface geometry.

The A–B junction points are, in effect, constrained to the liquid–liquid interface, due to the high incompatibility between the solvents and the prohibitive interaction energy penalty for chain crossover. Since the interface is narrow, compared to chain dimensions,[3,14] we can assume that each block is "tethered" by the junction point to an uncrossable surface. As the copolymer concentration at the interface increases, the chains overlap and two back-to-back, swollen brushes[3] are formed (see Figure 2).

We use a scaling approach to describe the polymer brush.[10,11] Correlations in chain configurations are introduced, in this approach, via a characteristic length scale which is a function of the local monomer concentration. The correlation length ξ (also referred to as "blob size"[11]), defines the range of excluded volume interactions. Over length scales smaller than ξ, chain configurations follow self-avoiding random-walk statistics, while over larger distances all interactions are screened. Scaling models of polymer brushes apply both to grafted chain systems, where the surface density is fixed, and to self-assembled structures, such as the microemulsion interface, where the surface density is controlled by thermodynamic equilibrium. They have been shown, by more rigorous methods,[15–17] to be comparatively accurate in the limit of high chain molecular weight.

Asymmetry in the copolymer molecular weight may lead to spontaneous curvature of the interface. Accurate accounting of the curvature effect on chain properties is essential in discussing systems where interface curvature may be of the same order of magnitude as chain dimensions,[17] such as polymer aggregates. Using simple geometrical considerations, it can be shown that the correlation length scales as[10–13]

$$\xi \sim a\sigma^{1/2}(r/R)^{D/2} \tag{1}$$

σ, the dimensionless surface density, is proportional to the number of chains per unit area. r is the radial distance from the droplet center, and R is the interface radius of curvature (see Figure 2). a is the segment size. D specifies the curvature dimensionality: $D = 0$ in planar geometry, $D = 1$ in cylinders, and $D = 2$ in spheres. (The symbol "$\sim$" is used throughout this paper to mean "equal within a numerical factor of order 1".)

The local volume fraction, ϕ, varies with the radius as

$$\phi(r) \sim \sigma^{2/3}(R/r)^{2D/3} \tag{2}$$

The thickness of the tethered brush is determined by the requirement that the concentration profile account for all the monomers in the brush:

$$Na^3 \sim \int_{V_{\text{chain}}} \phi(r)\, \mathrm{d}V \tag{3}$$

N is the number of monomers per chain and $\mathrm{d}V$ a volume element. The free energy density is proportional[11] to $1/\xi^3$, so that the free energy of a chain in a brush scales as

$$\frac{F}{kT} \sim \int_{V_{\text{chain}}} \frac{\mathrm{d}V}{\xi^3} \tag{4}$$

where k is Boltzmann's constant and T the temperature.

The free energy of a diblock copolymer chain, localized at the interface between two immiscible solvents, consists of three contributions, associated with the A block, the B block, and the interfacial region. Interfacial energy is proportional to the area per chain ($1/\sigma$) times γ, the dimensionless interfacial tension. Since the interfacial energy decreases with σ, it favors aggregation at the interface. The stretching energy of the copolymer blocks, which increases with copolymer surface density, arrests this tendency. We use the convention that N_B, the molecular weight of the B block, is smaller or equal to N_A, the molecular weight of the A block. The B chains are, therefore, located on the concave side of the interface. From eq 3 the thickness of the A and B brushes can be calculated and used to estimate the free energy of either block (eq 4). In spherical geometry, the free energy of a copolymer chain at a liquid–liquid interface scales as

$$\frac{F_{\text{int}}}{kT} \sim \gamma/\sigma + \sigma^{1/2}\frac{R}{a}\ln\left\{\frac{1 + N_A\sigma^{1/3}a/R}{1 - N_B\sigma^{1/3}a/R}\right\} \tag{5}$$

In the limit of large R eq 5 is reduced to the flat interface case.[7] The equilibrium layer properties are obtained by minimization of the free energy with respect to the two parameters interfacial curvature (R) and surface density (σ). We find that (see Appendix A)

$$\sigma \sim \left(\frac{\gamma}{N_B}\right)^{6/11} \frac{(x^2+1)^{6/11}}{(x+1)^{18/11}} \tag{6}$$

$$R/a \sim \gamma^{2/11} N_B^{9/11} \frac{(x^2+1)^{2/11}(x+1)^{5/11}}{(x-1)} \tag{7}$$

x is defined as N_A/N_B, a measure of the copolymer asymmetry. For nearly symmetrical copolymers, where $x \sim 1$, R is infinite. In this limit the surface density scales as $\{\gamma/(1+x)N_B\}^{6/11}$, in agreement with Cantor's results[7] for block copolymer lamellae. The free energy (per chain) scales as

$$\frac{F_{int}}{kT} \sim \gamma^{5/11} N_B^{6/11} \frac{(x+1)^{18/11}}{(x^2+1)^{6/11}} \tag{8}$$

The same procedure can be carried out for cylindrical geometry (see Appendix A). We find that the free energy of a chain in spherical geometry is lower than the free energy of a chain in a cylindrical one for all x values, as shown in Figure 3.

III. Onset of Microdomain Formation

We now discuss the system of a diblock copolymer mixed, at low concentration, with two immiscible solvents. Each of the solvents is capable of dissolving a limited amount of the diblock, a state referred to as "free chains". In the highly selective solvents considered, the insoluble block of the free chain collapses into a molten globule, surrounded by the solvated block "corona", as shown in Figure 2. The chemical potential of a free chain scales, approximately, as (see Appendix B)

$$\frac{\mu(\phi^{\alpha}_{AB})}{kT} \sim \ln \phi^{\alpha}_{AB} + N_B \tag{9a}$$

$$\frac{\mu(\phi^{\beta}_{AB})}{kT} \sim \ln \phi^{\beta}_{AB} + N_A \tag{9b}$$

where ϕ^{α}_{AB} and ϕ^{β}_{AB} are the volume fractions of copolymer in α and β, respectively. The reference state for each block is taken as that of infinite dilution in a good solvent.

As the copolymer concentration exceeds a threshold value, equivalent to the critical micelle concentration (cmc) in micellar solutions, chains assemble at the liquid–liquid interface. The free energy (per unit volume) of mixing AB, α, and β contains three contributions: from the free chains in α, the free chains in β, and the aggregates chains at the interface

$$\frac{\Delta F}{kT} = \phi_{\alpha}\frac{\phi^{\alpha}_{AB}}{N_A+N_B}\frac{\mu(\phi^{\alpha}_{AB})}{kT} + \phi_{\beta}\frac{\phi^{\beta}_{AB}}{N_A+N_B}\frac{\mu(\phi^{\beta}_{AB})}{kT} + \frac{\phi^{int}_{AB}}{N_A+N_B}\frac{F(\phi^{int}_{AB})}{kT} \tag{10}$$

ϕ_{α}, ϕ_{β}, and ϕ_{AB} are the volume fractions of α, β, and the copolymer, respectively, and ϕ^{int}_{AB} is the volume fraction of the copolymer at the liquid–liquid interface. We assume that ϕ_{AB} is much smaller than either solvent volume fraction and neglect the entropy of the emulsion droplets.

As the solvent–polymer mixture is approximately incompressible, two conservation laws can be applied:

$$\phi_{\alpha} + \phi_{\beta} + \phi_{AB} = 1 \tag{11}$$

$$\phi_{AB} = \phi_{\alpha}\phi^{\alpha}_{AB} + \phi_{\beta}\phi^{\beta}_{AB} + \phi^{int}_{AB} \tag{12}$$

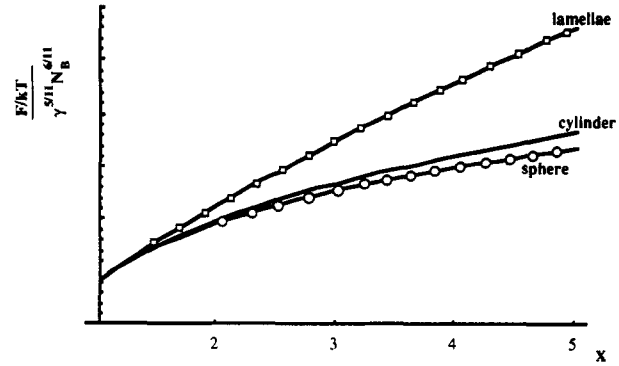

Figure 3. Free energy of spheres, cylinders, and lamellar interfaces, at equilibrium with excess solvent phases: (○) spheres, (—) cylinders, (□) lamellae.

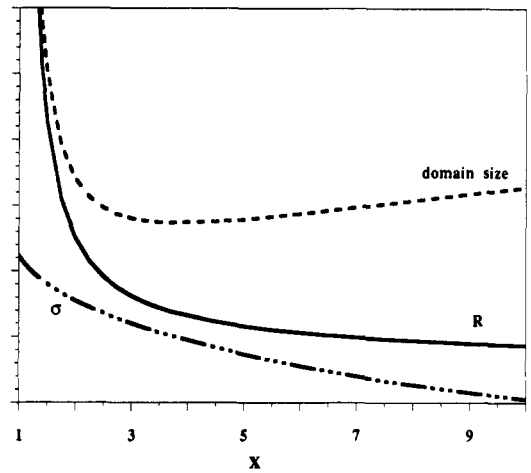

Figure 4. Spherical domain properties as a function of copolymer asymmetry, x. (– · · · –) Surface density, σ, in units of $(\gamma/N_B)^{6/11}$. (—) Interface radius, R/a, in units of $\gamma^{2/11}N_B^{9/11}$. (- - -) Domain size = $L_A + R$, in units of $\gamma^{2/11}N_B^{9/11}$.

The system free energy is, therefore, a function of four independent variables: ϕ^{α}_{AB}, ϕ^{β}_{AB}, σ, and R. Minimization with respect to these variables, in this order, and substitution of the values of eq 9 shows

$$\ln \phi^{\alpha}_{AB} \sim F_{int}/kT - (N_B + 1) \tag{13a}$$

$$\ln \phi^{\beta}_{AB} \sim F_{int}/kT - (N_A + 1) \tag{13b}$$

$$\partial(F_{int}/kT)/\partial\sigma = 0 \tag{13c}$$

$$\partial(F_{int}/kT)/\partial R = 0 \tag{13d}$$

The last two conditions are those minimizing the single interface energy, as shown in section II, so that the emerging emulsion phase is characterized by the surface density, radius, and free energy given in eqs 6–8. The surface density of the spherical domains, as a function of copolymer asymmetry, strongly decreases with x (Figure 4). The interface radius, however, decays rapidly to a nearly constant value. The overall domain size, which is equal to the sum of R and the corona thickness, obtains a minimum at a specific asymmetry ratio (about 3.75). Experiments measuring the domain size of a homologue series of block copolymer emulsions should enable testing of this prediction.

The concentration of free chains in each solvent phase is determined by eq 13a,b. When the copolymer concentration exceeds this solubility limit, chains migrate to the interface and emulsion domains form. The critical co-

polymer volume fraction is equal, therefore, to

$$\phi^*_{AB} = \phi^\alpha_{AB} + \phi^\beta_{AB} \sim \exp\{F_{int}/kT - N_B\} + \exp\{F_{int}/kT - N_A\} \quad (14)$$

F_{int}/kT (eq 8) is much smaller than either N_B or N_A, so that the concentration of free chains in either solvent is exceedingly low, and $\phi^*_{AB} \to \exp\{-N_B\}$.

In comparison, the critical concentration for micelle formation (cmc) scales as[18] $\exp\{N_B^{2/5}\gamma^{3/5} - N_B^{2/3}\gamma\} \to \exp\{-N_B^{2/3}\}$, quite higher than ϕ^*_{AB}.

The volume of the emulsion phase is defined as the volume of β solvent encapsulated in the droplet core. The core volume (neglecting the volume of B segments) scales as R^3. The number of droplets in the system is proportional to the copolymer volume fraction, ϕ_{AB}, divided by the volume of chains per droplet: $(\sigma R^2)N_B(1 + x)$. The emulsion phase volume fraction scales as

$$\bar{\phi}_\beta \sim \phi_{AB}\frac{R/a}{\sigma N_B(x+1)} \sim \phi_{AB}\left(\frac{N_B}{\gamma}\right)^{4/11}\frac{(x+1)^{12/11}}{(x-1)(x^2+1)^{4/11}} \quad (15)$$

Note that, as expected, the volume of emulsified β increases linearly with the copolymer volume fraction. In the case of symmetrical copolymers ($x = 1$) there is, in this model, no limit to the emulsion phase volume, since the lamellae spacing is unrestricted (a detailed analysis of the lamellar phase, where interactions between domains are considered, is given by Cantor[7]). $\bar{\phi}_\beta$ decreases with x for a given system composition and B block molecular weight.

In this regime spherical microemulsion domains coexist with the bulk β phase (Figure 1). The relative quantities of each phase are determined by eq 15 and the initial system composition. When all of the β solvent is encapsulated in the emulsion phase, that is, when $\bar{\phi}_\beta = \phi_\beta$, coexistence terminates. This limit corresponds to a copolymer volume fraction of

$$\phi^e_{AB} \sim \phi_\beta\left(\frac{\gamma}{N_B}\right)^{4/11}\frac{(x-1)(x^2+1)^{4/11}}{(x+1)^{12/11}} \quad (16)$$

ϕ^e_{AB} is referred to as the emulsification failure,[5] since at polymer concentrations lower than this value the solvent mixture cannot be completely emulsified. In an experiment where a second, inversely selective solvent (β) is slowly added to a copolymer micellar solution, the emulsification limit corresponds to the point at which a second phase of excess β droplets appears.[2] A systematic study of various block copolymer compositions and molecular weights should enable determination of the relationship between ϕ^e_{AB} and copolymer structure (x, N_B).

IV. Equilibrium Phase Diagram

We now investigate the equilibrium phase diagram of diblock copolymer–immiscible solvent mixtures, as a function of copolymer asymmetry and system composition. System composition is defined through the ratio of copolymer volume fraction, ϕ_{AB}, to the volume fraction of β solvent. The continuous phase, α, is taken as the majority component ($\phi_\alpha \gg \phi_{AB} + \phi_\beta$). Microdomain concentration is therefore low, and interactions between emulsion droplets need not be considered. We also neglect the entropy of the microdomain droplets and the presence of free chains, assuming that all copolymer chains are localized at the liquid–liquid interface.

For ϕ_{AB}/ϕ_β values lower than the emulsification limit (ϕ^e_{AB}/ϕ_β), the volume of the emulsion phase increases linearly with copolymer concentration (eq 15), and the chemical potential of the chains remains, approximately, unchanged. Above ϕ^e_{AB}, all the bulk core solvent phase is exhausted, and the emulsion phase volume is no longer free to vary, fixed by the initial value of ϕ_β. Further increase in the concentration of the copolymer changes the emulsion properties, since excess copolymer must aggregate at the liquid–liquid interface (the formation of micelles at equilibrium with emulsion droplets is unfavorable, as shown in Appendix B).

As in any construction of a phase diagram, we have to allow for phase coexistence. In this system, phases are distinguished by geometry: spherical, cylindrical, or lamellar. The constraint on the emulsion volume is expressed, for two coexisting phases, as

$$\phi_\beta = \epsilon\phi_\beta^{\,1} + (1-\epsilon)\phi_\beta^{\,2} \quad (17)$$

where ϵ is the fraction of chains in phase 1 (a single phase is equivalent to the case where $\epsilon = 0$ or 1). $\phi_\beta^{\,1}$ is the volume of β encapsulated in phase i, per chain

$$\phi_\beta^{\,i} \sim \phi_{AB}\frac{R_i/a}{\sigma_i N_B(x+1)} \quad (18)$$

for spheres or cylinders. In the case of lamellae, it has been shown by Cantor[7] that the preferred spacing between domains is equal to the lamellar thickness, so that

$$\phi_\beta^{lam} \sim \phi_{AB}\frac{L/a}{\sigma N_B(x+1)} \quad (19)$$

The free energy of the system is equal to

$$\frac{\Delta F}{kT} \sim \epsilon\frac{F_1(\sigma_1,R_1)}{kT} + (1-\epsilon)\frac{F_2(\sigma_2,R_2)}{kT} \quad (20)$$

where F_i is defined by eq 6 for spherical interfaces, or as

$$\frac{F_c}{kT} \sim \gamma/\sigma_c + \sigma_c^{1/2}\frac{R_c}{a}\{(1 + N_A\sigma_c^{1/3}a/R_c)^{3/8} - (1 - N_B\sigma_c^{1/3}a/R_c)^{3/8}\} \quad (21)$$

for cylindrical ones, and for lamellae as

$$F_l/kT \sim \gamma/\sigma_l + \sigma_l^{5/6}(N_A + N_B) \quad (22)$$

Minimization of the free energy, under the emulsion volume constraint, gives both the properties and the relative quantities of the different phases.

The first transition, between spherical and cylindrical droplets, occurs immediately above the emulsification failure concentration. Both phases retain (within a numerical constant) the radius and surface density of the initial emulsion phase, as defined by eq 5 and 6. The fraction of chains in the spherical droplets scales as

$$\epsilon \sim 2\frac{\phi_\beta}{\phi_{AB}}\left\{\frac{\phi^e_{AB}}{\phi_\beta}\right\} - 1 \quad (23)$$

so that $\epsilon = 1$ at $\phi_{AB} = \phi^e_{AB}$, linearly decreasing with increasing copolymer concentration. At the point where ϕ_{AB} is approximately $2\phi^e_{AB}$, the spherical droplets disappear and a single cylindrical phase remains. The cylinder radius is found to scale, using eq 18, as

$$R_c/a \sim \gamma^{2/5}N_B^{3/5}\left(\frac{\phi_\beta}{\phi_{AB}}\right)^{3/5}\frac{(x^2+1)^{2/5}(x+1)^{1/5}}{(x-1)^{2/5}} \quad (24)$$

R_c decreases with copolymer concentration to the point where the cylinder surface density is equal to the lamellar surface density, $(\gamma/(1+x)N_B)^{6/11}$, at which lamellae appear.

R_c of the coexistence phase scales as

$$R_c/a \sim \gamma^{2/11} N_B^{9/11} \frac{(x^2+1)^{2/5}}{(x^2-1)^{2/5}(x+1)^{2/11}} \quad (25)$$

and the fraction of chains in the cylindrical phase is

$$\epsilon \sim \frac{1}{1-\left\{\frac{(x^2+1)}{(x^2-1)}\right\}^{2/5}} \left\{ \left(\frac{\gamma}{N_B}\right)^{4/11} \left(\frac{\phi_\beta}{\phi_{AB}}\right) (1+x)^{7/11} - 1 \right\} \quad (26)$$

V. Discussion

We present a model for the phase diagram of the diblock copolymer in a mixture of incompatible and highly selective solvents, where microdomain geometry and size were determined by analysis of the interfacial layer.

The first emulsion phase to appear is that of spherical microdomains. For a given B block molecular weight, both the interface radius and surface density decrease with copolymer asymmetry. The critical concentration for aggregation is found to be lower than the critical micelle concentration (cmc),[18] scaling, for high molecular weight and degree of asymmetry, as $\exp\{-N_B\}$.

The aggregation number, defined as the number of chains per droplet, is an important, and measurable,[2] property of microemulsion droplets. Our model predicts an aggregation number scaling, in the limit of high x, as $N_B^{12/11}/x^{.10/11}$ From the numerical solution of a self-consistent-field model, Cogan et al.[8] predict that the aggregation number of spherical emulsion droplets should scale as $N_B^{1.6}/x^{0.9}$, for asymmetry ratios ranging between 3 and 14. The continuous phase (α) was taken, in these calculations, as a Θ solvent for the A corona chains. The agreement between the two models is quite good, considering the significant effect of solvent quality on A chain properties. Nagarajan and Ganesh[9] apply mean-field theory to study spherical emulsion droplets, in a mixture of two good solvents. They find that the aggregation number should scale as $N_B^{1.03}/x^{0.39}$, a much weaker dependence on x than in either scaling or SCF models. However, the concentration of both A and B monomers in the core and corona regions was assumed to be uniform, an assumption which has been lately shown[17] to be inaccurate when interface radii are comparable to chain dimensions, as is the case in highly asymmetric copolymer microdomains.

The spherical emulsion phase volume increases linearly with copolymer concentration, until all excess β phase is exhausted. Further addition of copolymer leads to the appearance of a coexisting cylindrical phase. The volume of the spherical emulsion phase decreases linearly with copolymer concentration, until all is exhausted and only cylindrical droplets remain. The curvature of the single-phase cylindrical aggregates increases with ϕ_{AB}. Lamellae appear at the point where the surface density of the cylindrical phase is equal to that of the lamellae.

The order of domain appearance is similar to that predicted for block copolymer–homopolymer blends,[5,6] though quantitative comparison is impossible due to the qualitative nature of the scaling model and the different behavior of chains in bulk and in solution. We emphasize that the order of phase appearance was determined after normalizing the free energies of the phases to the value of lamellae at $x = 1$. Since, by necessity, the appropriate prefactors of the scaling free energies would have obtained the same end, their inclusion is unnecessary and would not change any of this analysis' conclusions. Geometrical prefactors, omitted from eq 18 and 19, may shift the phase boundaries but not alter phase properties or sequence. It should be noted, however, that the phase diagram presented here is restricted to the geometries examined, and the appearance of other phases, such as bicontinuous structures, cannot be predicted.

We have neglected possible coexistence between microemulsion droplets and micelles. However, as noted in section III, the critical copolymer concentration for the onset of micellization (cmc) is higher than the critical concentration for microemulsion formation, ϕ^*_{AB}. This is in agreement with experimental data[2] where it has been observed that the cmc was appreciatively higher than the critical aggregation concentration for "swollen micelles", i.e., microemulsions, when a second, inversely selective solvent was added. Also, there was no evidence of micelle–swollen micelle coexistence. Emulsion domains would appear, therefore, before micelles do. The chemical potential of a chain in a micelle scales,[18,19] for highly asymmetric copolymers, as $N_B^{2/5}\gamma^{3/5} + N_B\Delta\chi$, where the second contribution is due to matching of reference states (between melt conditions and that of the solvated state). The free energy of a highly asymmetric chain in a microemulsion droplet is therefore lower than that of a chain in a micelle (see eq 8), unless $\Delta\chi N_B^{5/11} < \gamma^{5/11}(x+1)^{18/11}/(x^2+1)^{6/11}$. The probability of micelle coexistence is therefore negligible in most polymer systems, unless x is on the order of N_B.

Systematic experimental investigation of the size dependence of microemulsion domains on copolymer molecular weight and concentration may be guided by this analysis, with the aim of ascertaining the validity of the basic physics contained in this model.

Acknowledgment is made to the donors of the Petroleum Research Fund, administered by the American Chemical Society, for partial support of this research. Partial support was also received, with appreciation, from the National Science Foundation (NSF/CTS-9107025, Interfacial Transport and Separations Program [CTS] and Polymers Program [DMR]). We thank A. Halperin for suggesting this problem to us and for helpful and exciting discussions.

Appendix A

The free energy of a spherical interface scales as

$$\frac{F_s}{kT} \sim \frac{\gamma}{\sigma} + \sigma^{1/2}\frac{R}{a} \ln\left\{\frac{1+N_A\sigma^{1/3}a/R}{1-N_B\sigma^{1/3}a/R}\right\} \quad (5)$$

Minimization with respect to R yields

$$0 = \frac{1}{a}\sigma^{1/2} \ln\frac{1+N_A\sigma^{1/3}a/R}{1-N_B\sigma^{1/3}a/R} - \sigma^{1/2}\frac{R}{a}\left\{\frac{N_A\sigma^{1/3}a/R^2}{(1+N_A\sigma^{1/3}a/R)} + \frac{N_B\sigma^{1/3}a/R^2}{(1-N_A\sigma^{1/3}a/R)}\right\} \quad (A.1)$$

and with respect to σ

$$0 = -\gamma/\sigma^2 + 1/2\frac{R}{a}\sigma^{-1/2} \ln\frac{1+N_A\sigma^{1/3}a/R}{1-N_B\sigma^{1/3}a/R} + 1/3R^{1/2}\frac{R}{a}\left\{\frac{N_A\sigma^{-2/3}a/R}{(1+N_A\sigma^{1/3}a/R)} + \frac{N_B\sigma^{-2/3}a/R}{(1-N_B\sigma^{1/3}a/R)}\right\} \quad (A.2)$$

Defining a new variable, y, as $N_B\sigma^{1/3}a/R$, eq A.1 and A.2

can be rearranged to show

$$\ln \frac{1+xy}{1-y} = \frac{xy}{1+xy} + \frac{y}{1-y} \tag{A.3}$$

so that y is a function of x, the ratio between block molecular weight, only. Equation A.3 cannot be solved analytically, especially since some numerical coefficients, or order 1, have been neglected throughout the derivation. However, a numerical solution shows that $y(x)$ has an approximate form of $(x-1)/(1+x)$: At high asymmetry ratios, $y \sim 1$, while at low ratios $y \sim 0$. Obviously, this fit is not unique, but it does yield the correct limit behavior. From the definition of y

$$R/a \sim \frac{N_B \sigma^{1/3}(1+x)}{x-1} \tag{A.4}$$

and, combined with eq A.2, we find

$$\sigma \sim \left(\frac{\gamma}{N_B}\right)^{6/11} \frac{(2x^2+2)^{6/11}}{(x+1)^{18/11}} \tag{6}$$

For $x = 1$, $\sigma = (\gamma/2N_B)^{6/11}$, in agreement with Cantor's[7] predictions for symmetrical copolymer lamellae. For convenience, we omit the prefactor of $2^{6/11}$ in eq 6 and the following derivations.

The same procedure is carried out for cylindrical interfaces. To enable direct numerical comparison between the free energy of the different phases, we normalize all three geometries to the same value for $x = 1$, the lamellar phase: $F_s(x=1) = F_c(x=1) = F_l$.

Appendix B

The chemical potential of a polymer chain is equal to[3,11,18]

$$\frac{\mu}{kT} = \ln \phi + \frac{F_{\phi=0}}{kT} \tag{B.1}$$

where $F_{\phi=0}$ is the free energy of a chain at infinite dilution, compared to a reference state. The reference state chosen for each block is that of an isolated chain in good solvent. The configuration of the copolymer in α solvent is that of a solvated A corona, surrounding a collapsed B block core (and vice versa for chains in β solvent). Therefore, the free energy of the solvated block in an isolated chain is approximately equal to that of the reference state and does not affect the chemical potential. Two terms remain: the interfacial energy between the collapsed block globule and the solvent and the energy of the B core, compared to the reference state.[18] It is reasonable to assume that, due to the high incompatibility between α and B, no solvent penetrates and the core is composed of B segments in the melt state, so that $R_c \sim aN_B^{1/3}$.

The difference in interaction energy between an isolated chain in good solvent and a chain in the melt is proportional to the difference in pairwise interaction energy between the two states, $\chi_{bulk} - \chi_{good}$, times the number of segments, where χ is the Flory–Huggins parameter. In a good solvent, χ is negative, while in bulk $\chi = 0$. Therefore, the energy of an isolated chain can be written as

$$\frac{F_{\phi=0}}{kT} \sim \gamma' N_B^{2/3} + \Delta\chi N_B \tag{B.2}$$

γ' is the (dimensionless) interfacial tension between B in bulk and the α solvent (not necessarily equal to γ, the interfacial tension between the two solvents).

Values of interfacial tension for polymer-incompatible solvents are of order kT (ranging, at room temperature, between 1 and 5 for most polymer–solvent pairs). For high B block molecular weights, γ' is much smaller than $N_B^{1/3}$, and eq A.2 is dominated by the interaction term. The chain chemical potential scales as

$$\frac{\mu(\phi_{AB}^{\alpha})}{kT} = \ln \phi + N_B \tag{B.3}$$

References and Notes

(1) Rigby, D.; Roe, R. J. *Adv. Polym. Sci.* **1987**, *82*, 105.
(2) Cogan, K. A.; Gast, A. P. *Macromolecules* **1990**, *23*, 745.
(3) Halperin, A.; Tirrell, M.; Lodge, T. P. *Adv. Polym. Sci.* **1991**, *100*, 31.
(4) Scott, C. Ph.D. Thesis, University of Minnesota, Minneapolis, MN, 1991.
(5) Wang, Z. G., Safran, S. A. *J. Phys. (Fr.)* **1990**, *51*, 185.
(6) Leibler, L. *Makromol. Chem., Macromol. Symp.* **1988**, *16*, 1.
(7) Cantor, R. *Macromolecules* **1981**, *14*, 1186.
(8) Cogan, K. A.; Leermakers, F. A.; Gast, A. P. *Langmuir* **1992**, *8*, 429.
(9) Nagarajan, R.; Ganesh, K. *Macromolecules* **1989**, *22*, 4312.
(10) Alexander, S. *J. Phys. (Fr.)* **1976**, *38*, 977.
(11) de Gennes, P.-G. *J. Phys. (Fr.)* **1976**, *37*, 1445; *Scaling Concepts in Polymer Physics*; Cornell University Press: Ithaca, NY, 1979.
(12) Daoud, M.; Cotton, J. P. *J. Phys. (Fr.)* **1982**, *43*, 531.
(13) Birshtein, T. M.; Zhulina, E. B.; Khokhlov, A. R.; Yurasova, T. A. *J. Polym. Sci. USSR* **1987**, *29*, 1293.
(14) Noolandi, J.; Hong, K. M. *Macromolecules* **1983**, *16*, 1443.
(15) Milner, S. T. *J. Chem. Soc., Faraday Trans.* **1990**, *86*, 349.
(16) Murat, M.; Grest, G. S. *Macromolecules* **1991**, *24*, 704. Grest, G. S.; Kremer, K.; Witten, T. A. *Macromolecules* **1987**, *20*, 1376.
(17) Dan, N.; Tirrell, M. *Macromolecules* **1992**, *25*, 2890.
(18) Marques, C.; Joanny, J. F.; Leibler, L. *Macromolecules* **1988**, *21*, 1051.
(19) Halperin, A. *Macromolecules* **1987**, *20*, 2943.